

Na[Li(NH₂BH₃)₂] – the first mixed-cation amidoborane with unusual crystal structure†‡

Karol J. Fijalkowski,^a Radostina V. Genova,^b Yaroslav Filinchuk,^{c,d} Armand Budzianowski,^b Mariana Derzsi,^b Tomasz Jaron,^a Piotr J. Leszczyński^b and Wojciech Grochala^{*a,b}

Received 29th October 2010, Accepted 10th January 2011

DOI: 10.1039/c0dt01491e

We describe the successful synthesis of the first *mixed-cation* (pseudoternary) amidoborane, Na[Li(NH₂BH₃)₂], with theoretical hydrogen capacity of 11.1 wt%. Na[Li(NH₂BH₃)₂] crystallizes triclinic (*P* $\bar{1}$) with *a* = 5.0197(4) Å, *b* = 7.1203(7) Å, *c* = 8.9198(9) Å, α = 103.003(6)°, β = 102.200(5)°, γ = 103.575(5)°, and *V* = 289.98(5) Å³ (*Z* = 2), as additionally confirmed by Density Functional Theory calculations. Its crystal structure is topologically different from those of its orthorhombic LiNH₂BH₃ and NaNH₂BH₃ constituents, with distinctly different coordination spheres of Li (3 N atoms and 1 hydride anion) and Na (6 hydride anions). Na[Li(NH₂BH₃)₂], which may be viewed as a product of a Lewis acid (LiNH₂BH₃)/Lewis base (NaNH₂BH₃) reaction, is an important candidate for a novel lightweight hydrogen storage material. The title material decomposes at low temperature (with onset at 75 °C, 6.0% mass loss up to 110 °C, and an additional 3.0% up to 200 °C) while evolving hydrogen contaminated with ammonia.

Introduction

Amidoboranes (amidotrihydroborates) constitute a well researched family of ammonia borane^{1–2} [NH₃BH₃] derivatives consisting of metal cations and amidoborate anions (NH₂BH₃[–], for short, AB) (Table 1). The first amidoborane (sodium salt, NaAB) was synthesized by Schlesinger and Burg as early as in 1938,³ but this family of compounds was then forgotten for over half a century. Rediscovered in the late 1980s, the amidoboranes of several mono- and di-valent metals (Li, Na, K, Eu, Yb) were investigated by the group of Shore.^{4–6} The possibility of using amidoboranes as reducing agents in organic chemistry has been discussed.⁷ Only recently have amidoboranes gained importance in the context of research on hydrogen storage. Lithium^{6–8} sodium,^{9–10} potassium,^{6,11} and strontium¹² amidoboranes exhibit low temperature hydrogen desorption (~80–90 °C) while calcium amidoborane^{13,14} decomposes thermally at slightly higher temperatures (over 105 °C). Recently the first amidoborane

Table 1 Comparison between the known single-cation amidoborane phases and novel mixed-cation amidoborane of lithium and sodium (H_%: theoretical gravimetric hydrogen content; Dec.: temperature of decomposition; [*]: present work)

Cation	Formula	Symbol	H _%	Dec.	Ref.
Lithium	LiNH ₂ BH ₃	LiAB	13.5%	92 °C	8
Sodium	NaNH ₂ BH ₃	NaAB	9.4%	89 °C	8
Potassium	KNH ₂ BH ₃	KAB	7.3%	80 °C	6
Calcium	Ca(NH ₂ BH ₃) ₂	Ca(AB) ₂	10.0%	105 °C	13
Strontium	Sr(NH ₂ BH ₃) ₂	Sr(AB) ₂	6.8%	93 °C	12
Yttrium	Y(NH ₂ BH ₃) ₃	Y(AB) ₃	8.4%	80 °C	15
Europium	Eu(NH ₂ BH ₃) ₂	Eu(AB) ₂	4.7%	?	5
Ytterbium	Yb(NH ₂ BH ₃) ₂	Yb(AB) ₂	4.3%	?	5
Li + Na	Na[Li(NH ₂ BH ₃) ₂]	NaLi(AB) ₂	11.1%	75 °C	[*]

of a trivalent metal, yttrium, was synthesized, and it proved to be much less thermally stable than all other known amidoboranes (it spontaneously decomposes at room temperature over a few days, and very quickly above 80 °C).¹⁵ Unsuccessful attempts to synthesize lightweight aluminium amidoborane¹⁶ and magnesium amidoborane^{17,18} were also reported. It is puzzling that the formation of Na[Li(NH₂BH₃)₂] was overlooked in the previous study on various milled mixtures of NaH, LiH and AB, which aimed at elimination of ammonia evolution.¹⁹

Unfortunately, the raw materials [LiAB, NaAB, Ca(AB)₂, Sr(AB)₂, or Y(AB)₃] are not directly suited for fuel cell applications due to evolution of ammonia during their thermal decomposition^{10,12,13,15,20,21} (NH₃ is a poison for fuel cell membranes and Pt catalysts even at the ppm level).²² The lack of reversibility of the thermal decomposition process and unfavourable thermodynamics are other concerns.

^aFaculty of Chemistry, University of Warsaw, Pasteura 1, 02-093, Warsaw, Poland. E-mail: wg22@cornell.edu

^bICM, University of Warsaw, Pawińskiego 5a, 02-106, Warsaw, Poland

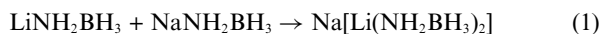
^cSwiss-Norwegian Beam Lines at ESRF, BP-220, 38043 Grenoble, France

^dInstitute of Condensed Matter and Nanosciences, Université Catholique de Louvain, place L. Pasteur 1, B-1348 Louvain-la-Neuve, Belgium

† This work is dedicated to Prof. Marek Niezgodka at his 60th birthday.

‡ Electronic supplementary information (ESI) available: FTIR spectra, results of Elemental Combustion Analysis of all composites, details of the thermal decomposition of LiAB reference samples, comparison of calculated and experimental unit cells of NaLiAB₂. CCDC reference number 795163. For ESI and crystallographic data in CIF or other electronic format see DOI: 10.1039/c0dt01491e

So far only the *single-cation* amidoboranes of many different metals have been synthesized and characterized, with no *mixed-cation* (pseudoternary) amidoboranes reported so far. It is conceivable, however, that the Lewis acid–Lewis base reactions between an amidoborane of the lightest and smallest (Li^+) and amidoboranes of the heavier alkali metal cations, for example:



will alter the thermal stability and other properties of the mixed-cation phase with respect to its pseudobinary constituents, similarly to what is observed for hydride,²³ aluminohydride^{24–26} and borohydride^{27–29} materials. In particular, thermodynamically facile acid–base reactions should lead to an increased thermodynamic and thermal stability, which in turn should be beneficial in the case of inherently thermodynamically unstable amidoboranes.

In the current study we are testing this simplistic concept in relation to amidoborane hydrogen storage materials and we describe synthesis and characterization of the first bimetallic amidoborane, $\text{Na}[\text{Li}(\text{NH}_2\text{BH}_3)_2]$. The theoretical total hydrogen capacity of the novel compound is 11.1 wt% (gravimetric) and 114.4 g l⁻¹ (volumetric). $\text{NaLi}(\text{AB})_2$ may be synthesized *via* a fast, single-pot mechanochemical solid–solid reaction similar to the synthesis of single-cation amidoboranes of lithium and sodium (eqn (2)).



We report crystal structure of the title compound as well as details of its thermal decomposition. $\text{NaLi}(\text{AB})_2$ contains polymeric $[\text{Li}(\text{AB})_2^-]_2$ anions stacked along the *a* crystallographic axis and separated by isolated Na^+ cations, and it is very different from the crystal structures for LiAB and NaAB . Indeed, $\text{NaLi}(\text{AB})_2$ is the first example of an inorganic mixed lithium–sodium compound where, facilitated by topology of amidoborate anion, stronger Lewis bases (NH_2) coordinate a stronger Lewis acid (Li^+) while allowing weaker Lewis bases (BH_3) to bind to a weaker Lewis acid (Na^+). In contrast to its anticipated increased thermodynamic stability, $\text{NaLi}(\text{AB})_2$ is slightly less thermally stable (by *ca.* 10 °C) than its pseudobinary constituents.

Experimental

1. Synthesis

$\text{Na}[\text{Li}(\text{NH}_2\text{BH}_3)_2]$ was obtained by disk milling of the dry substrates: LiH (95%, Sigma Aldrich), NaH (95%, Sigma Aldrich) and NH_3BH_3 of the highest commercially available purity (98%, JSC Aviabor), in a 1 : 1 : 2 ratio following eqn (2). An attempted alternative synthesis following eqn (1) involving milling of pre-formed LiAB and NaAB failed to give the desired product. The amorphous composite obtained has inferior properties to $\text{Na}[\text{Li}(\text{AB})_2]$ as far as hydrogen storage and purity of evolved H_2 are considered.

Milling was carried out in a Testchem high energy disk mill with a bowl made of tungsten carbide. To avoid thermal decomposition of the product during the synthesis, the milling process was carried out with breaks for cooling. The substrates were milled three times for 3 min with two 5 min breaks. The product was cooled down and analysed without further purification.

All operations with substrates and products were performed in an argon filled Labmaster DP MBRAUN glovebox ($\text{O}_2 < 1.0$ ppm; $\text{H}_2\text{O} < 1.0$ ppm).

2. TGA/DSC/EGA

Thermal decomposition (mass loss, heat flow) was investigated using an STA 409 simultaneous thermal analyzer from Netzsch, in the temperature range 30–350 °C. The STA allows for simultaneous thermogravimetric analysis (TGA), differential scanning calorimetry (DSC) and evolved gas analysis (EGA). The samples were loaded into alumina crucibles and a heating rate of 10 K min⁻¹ and 99.9999% Ar purge gas was used. The evolved gases were analyzed with a Q-MS 403 C Aëolos mass spectrometer from Pfeiffer-Vacuum (connected to the STA *via* a quartz capillary) and a Vertex 80v infrared spectrometer from Bruker (its gas cell connected to the STA *via* a PTFE tube). Both transfer lines were preheated to 200 °C to avoid condensation of residues.

3. XRD

The crystallinity and purity of the samples and the products of their thermal decomposition were investigated using a D8 Discover diffractometer from Bruker with $\text{Cu-K}\alpha_1$ and $\text{Cu-K}\alpha_2$ radiation ($\lambda \approx 1.5406$ Å) at an intensity ratio of *ca.* 2 : 1, for a typical angle range from 3 to 90° and the step size lower than 0.02°. The Vantec detector has been used to record the diffraction from the samples. Every sample was sealed in a 1.0 mm thick quartz capillary under an Ar atmosphere.

XRD Synchrotron powder diffraction data in the 3.0–23.3° 2θ range were collected at the Swiss-Norwegian beamline (BM1A) ($\lambda = 0.73808$ Å) at the European Synchrotron Radiation Facility (ESRF) (Grenoble, France) using a MAR345 image plate detector. The sample-to-detector distance and the image plate tilt angles were calibrated using a standard LaB6 sample. The sample was filled under argon into a thin-walled glass capillary. A powder pattern for structure solution was collected at room temperature. In addition, in order to observe *in situ* a decomposition of $\text{NaLi}(\text{AB})_2$ the temperature was varied from 31.5 to 111.7 °C. Temperature was increased at a rate of 4 K min⁻¹ rate using an Oxford Cryostream 700+. Every 2 min a dataset was collected, with an exposure time of 30 s, followed by a readout of 90 s. *In situ* diffraction measurements have shown that the disappearance of crystalline $\text{NaLi}(\text{AB})_2$ started at ~47 °C and was completed at ~63 °C. The two-dimensional diffraction images were azimuthally integrated using the Fit2D program.³⁰

4. Structure determination from X-ray diffraction data

Impurities and phase identification. Diffractograms recorded using $\lambda = 1.5406$ Å radiation have been used for validation, completion and refinement of the structure model using Materials Studio³¹ (TREOR90,³² DICVOL91,²⁹ ITO15,³³ X-Cell³⁴) and TOPAS³⁵ (LSI-Index³⁶). Two impurities have been found: WC in $P6m_2$ ($a = b = 2.906(3)$ Å, $c = 2.8387(4)$ Å) and an unknown impurity phase with unit cell parameters $a = 4.736(2)$ Å, $b = 4.298(3)$ Å, $c = 4.023(4)$ Å, $\alpha = 87.3(7)^\circ$, $\beta = 112.7(3)^\circ$, $\gamma = 115.7(9)^\circ$, but unknown space group and structure (further denoted as ‘P1’). All samples of $\text{NaLi}(\text{AB})_2$ contain these two impurities. Reflexes of this triclinic phase were identified from a set of syntheses using

different milling times; depending on the milling time, *P1* phases were present in a different ratio to the main $\text{NaLi}(\text{NH}_2\text{BH}_3)_2$ phase, which allowed for identification of two subsets of reflexes in XRDP. The whole powder pattern was then decomposed according to Pawley³⁷ and Le Bail³⁸ methods in TOPAS while applying a Fundamental Parameters Approach³⁹ as a function of profile shape.

Structure solution and Rietveld refinement. 13 diffraction peaks from synchrotron data were indexed by Dicolv⁴⁰ in a triclinic cell, $M(13) = 77.2$. All attempts to index in a higher symmetry failed. The structure was solved in the space group $P\bar{1}$ by global optimization in direct space by the program FOX.⁴¹ Positions of one Li, one Na atom and the positions and orientation of two AB groups were optimized, applying rigid body constraints for the geometry of AB anions and anti-bump restraints preventing the units coming too close. Examination of the resulting structure and analysis by Platon⁴² did not find a higher crystallographic symmetry. This model has been used for structure refinement using Rietveld for a multicomponent mixture of two crystal structures (WC , $\text{NaLi}(\text{NH}_2\text{BH}_3)_2$) and the third unknown impurity phase *P1*. The anti-bump penalties and the rigid body assumption for two independent NH_2BH_3^- anions have been applied. The following bond length limits have been applied for the rigid bodies: B–N (1.51–1.61 Å), N–H (1.00–1.10 Å) and B–H (1.22–1.32 Å). Values of angles H–N–H, H–B–H, B–N–H and N–B–H were allowed to vary between 108° and 111° while all torsion angles were set free. The anti-bump penalties were as follows: for Li atoms to B (2.6 Å), Li (2.7 Å), H (1.9 Å), N (2.9 Å), for Na atoms to H (2.6 Å), B (3.0 Å), for N atoms: N (2.9 Å) and B (1.34 Å), with an additional one for H2...H7 contact (2.2 Å).

The structure of $\text{NaLi}(\text{AB})_2$ has been refined in TOPAS using synchrotron data with modified Thompson–Cox–Hastings pseudo-Voigt “PV_TCHZ” functions of profile shape for Rietveld structure refinement.⁴³ The final R_{Bragg} parameters are: 2.07% for $\text{NaLi}(\text{AB})_2$ and 1.66% for WC; the quantitative phase content analysis⁴⁴ yields: WC (5.2(1) wt%), $\text{NaLi}(\text{AB})_2$ (94.8(1) wt%) (content of the unknown *P1* minority phase was set to 0%).

Further details of the crystal structure may be obtained from the ESI† and from Fachinformationszentrum Karlsruhe, 76344 Eggenstein-Leopoldshafen, Germany (fax: (+49)7247-808-666; e-mail: crysdata@fizkarlsruhe.de) on quoting the appropriate CSD number CSD-422190.

4. FTIR

All substrates, products and thermally decomposed samples were characterized with infrared absorption spectroscopy in KBr pellets using a Vertex 80v vacuum FTIR spectrometer from Bruker.

5. Elemental composition analysis

Samples were analyzed for N, H and trace C content with an elemental combustion (240 Perkin Elmer) analyzer at a detectability level of 0.2 wt% and a typical uncertainty of 0.3 wt% for each element. Two independent analyses were performed with differences between the measurements reaching no more than 0.2 wt% for each element. The numbers shown in this work are the mean of the two values (or sometimes more).

6. Density Functional Theory calculations

Our solid state calculations were performed on $1 \times 1 \times 1$ cell (32 atoms) using a projector-augmented wave method (PAW)⁴⁵ as implemented in the Vienna *ab initio* Simulation Package (VASP).⁴⁶ The model structure was constructed from preliminary experimental data. Parameters for full unit cell relaxation: electronic convergence 1×10^{-7} eV, ionic convergence 1×10^{-6} eV, $1 \times 2 \times 3$ k-point mesh (Monkhorst–Pack scheme was used). Valence electrons were described by plane waves with a kinetic energy cutoff of 700 eV providing good convergence of electronic energy, while core electrons by relativistic ultrasoft Vanderbilt type pseudopotentials. LDA as well as a GGA-PBE approach was applied for the exchange-correlation functional, GGA-PBE resulting in a much better reproduction of the unit cell volume (282.6 Å³) than LDA (236.57 Å³). The former method was used for subsequent DOS calculations (*cf.* ESI†).

Results and discussion

1. Crystal structure

$\text{NaLi}(\text{AB})_2$ obtained by disk milling is a low-density powder. Powder X-ray patterns of LiAB, NaAB, $\text{NaLi}(\text{AB})_2$ and the product(s) of its thermal decomposition at 110 °C, are shown in Fig. 1. The diffractogram of $\text{NaLi}(\text{AB})_2$ does not contain any reflections from the single-cation amidoboranes of Li and Na, confirming quantitative conversion to the product. The unknown impurity phase *P1* and a small amount of strongly-diffracting WC are present in the sample as an effect of abrasion of the mill material; LiH and NaH are absent. All remaining reflections can be assigned to crystalline $\text{NaLi}(\text{AB})_2$.⁴⁷

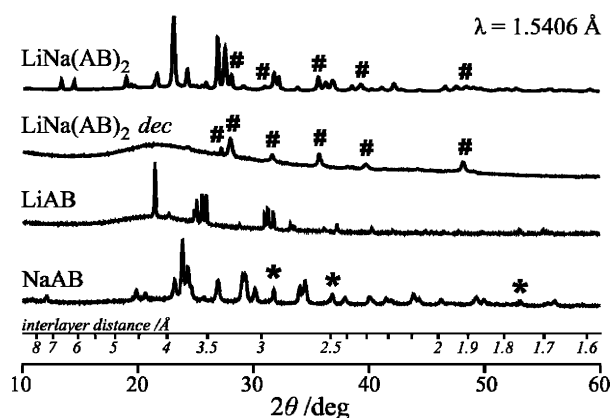


Fig. 1 Comparison of X-ray powder diffraction data (CuK radiation) for $\text{LiNa}(\text{AB})_2$ (top) and single-cation amidoboranes of lithium and sodium (bottom). Reflections from NaH (*) and WC (#) are marked.

The synchrotron diffraction pattern of $\text{NaLi}(\text{AB})_2$ was indexed based on a triclinic unit cell (Fig. 2). The subsequent Rietveld refinement yielded the following $P\bar{1}$ (No. 2) unit cell with parameters $a = 5.0197(4)$ Å, $b = 7.1203(7)$ Å, $c = 8.9198(9)$ Å, $\alpha = 103.003(6)^\circ$, $\beta = 102.200(5)^\circ$, $\gamma = 103.575(5)^\circ$, and volume of $V = 289.98(5)$ Å³ ($Z = 2$, hence 144.99(3) Å³ per formula unit). The arithmetic mean of the formula unit volumes of LiAB and NaAB is 141.24 Å³, hence the volume of $\text{LiNa}(\text{AB})_2$ is *ca.* 2.0% larger than the expected value.⁴⁸

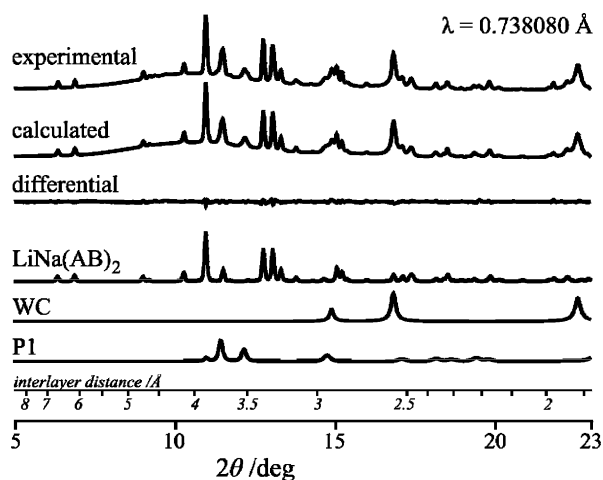


Fig. 2 Rietveld decomposition of the diffractogram of $\text{NaLi}(\text{AB})_2$ (synchrotron radiation) showing all phases present in the sample: $\text{NaLi}(\text{AB})_2$, WC, and unknown *P1* phase (see text).

$[\text{Li}(\text{AB})_2]^-$ anions polymerized into 1D infinite $[\text{Li}(\text{AB})_2]^-_n$ chains *via* short $\text{Li}\dots\text{H}$ interactions, and stacked along the *a* crystallographic axis, are present in the crystal structure of $\text{NaLi}(\text{AB})_2$ (Fig. 3); the chains are separated by isolated Na^+ cations which serve as counterions. Li^+ cations are coordinated by three N atoms of amine groups (at 2.157 Å, 2.161 Å, 2.261 Å) with one hydride from the BH_3 group (at 1.875 Å) completing lithium's coordination sphere to a distorted tetrahedron. The $[\text{Li}_2\text{N}_2]$ units, similar to the $[\text{Li}_2\text{O}_2]$ units seen for lithium fluorosulfate,⁴⁹ may be distinguished in the crystal structure. The first coordination sphere of Na^+ cation contains six hydride anions from BH_3 groups (at 2.299 Å, 2.316 Å, 2.344 Å, 2.432 Å, 2.484 Å, 2.513 Å) in a quite irregular arrangement. The crystal structure of $\text{NaLi}(\text{AB})_2$ thus has a very clear ionic aspect with well-defined Na^+ and $[\text{Li}(\text{AB})_2]^-$ sublattices, making it very different from the crystal structures of orthorhombic α -LiAB (and also very likely isostructural NaAB), and β -LiAB (where each alkali metal cation is coordinated by both

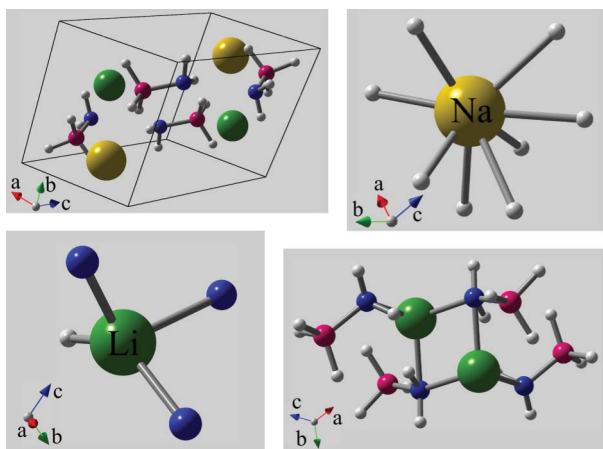


Fig. 3 The crystal structure of $\text{NaLi}(\text{AB})_2$: (left top) crystallographic unit cell; (right top) the first coordination sphere of Na^+ at <2.6 Å; (left bottom) the first coordination sphere of Li^+ at <2.3 Å; (right bottom) projection emphasizing the presence of dimeric $[\text{Li}(\text{AB})_2]^-$ anions. H white, B red, N blue, Li green, Na yellow. Positions of light H atoms are tentative and should be taken with care.

Table 2 Comparison between the experimental and theoretical (DFT) unit cell parameters of $\text{NaLi}(\text{NH}_2\text{BH}_3)_2$. Uncertainties were omitted. For comparison of fractional atomic coordinates see the ESI[†]

Method	<i>a</i> /Å	<i>b</i> /Å	<i>c</i> /Å	α (°)	β (°)	γ (°)	<i>V</i> /Å ³
Exp.	5.020	7.120	8.920	103.0	102.2	103.6	289.98
DFT	5.035	7.102	8.768	102.5	102.7	105.1	282.58

N and H electron density donors and where charge separation is absent).

Indeed, $\text{NaLi}(\text{AB})_2$ is the first example⁵⁰ of an inorganic mixed lithium–sodium compound where, facilitated by the topology of the amidoborate anion, and by the difference of ionic radii of Li^+ and Na^+ , all stronger Lewis bases (NH_2) coordinate to a stronger Lewis acid (Li^+) and simultaneously a weaker Lewis acid (Na^+) is found in the homoleptic environment of weaker Lewis bases, BH_3 (recollect that hydrogen has a somewhat anionic, *i.e.* hydridic, character in B_2H_6 and even more so in borohydrides). In other words, $\text{Na}[\text{Li}(\text{NH}_2\text{BH}_3)_2]$ shows coordination of the more electron-rich nitrogen end of two amidoborane anions to the more electrophilic Li^+ as compared to the less electrophilic Na^+ . Such is a structural impact of the solid state Lewis acid–Lewis base reaction where NaAB donates its amidoborane anions to more acidic LiAB.

DFT calculations confirm the crystal structure of $\text{Na}[\text{Li}(\text{AB})_2]$ with maximum deviation between the calculated and experimental lattice parameters of 2% (Table 2).

2. Infrared absorption spectra

The FTIR absorption spectrum of $\text{NaLi}(\text{AB})_2$ is shown in Fig. 4; band positions are listed in the ESI.[†] Weak sharp bands above 3600 cm^{-1} represent the small amount of LiOH and NaOH impurities formed during reaction of the sample with traces of atmospheric moisture during FTIR measurements. X-Ray analysis of samples kept in an argon atmosphere shows that neither LiOH nor NaOH is present in considerable amounts.

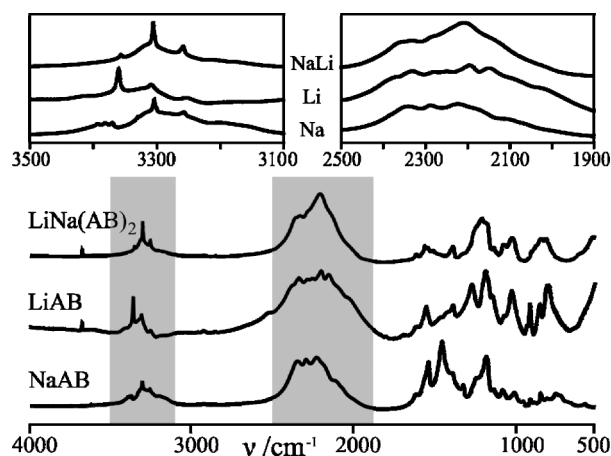


Fig. 4 Comparison of the FTIR spectra of $\text{LiNa}(\text{AB})_2$ and of the constituent single-cation amidoboranes of lithium and sodium. The ranges marked in grey are shown magnified at the top.

The IR spectrum of $\text{LiNa}(\text{AB})_2$ consists of several distinct absorption bands in the NH stretching (3000–3400 cm^{-1}), BH stretching (1800–2600 cm^{-1}), BN stretching (1300–1500 cm^{-1}),

NH deformation (1500–1610 cm⁻¹), and BH deformation (1000–1270 cm⁻¹) regions, as typical for all amidoboranes. The main BH stretching band, centered at 2211 cm⁻¹, is sharper and less structured than those in the spectra of the single-cation analogues. At first sight, the NH stretching region of LiNa(AB)₂ resembles a combination of the spectra measured for LiAB and NaAB (see magnified region, Fig. 4), albeit of weak intensity. This is actually a coincidence since the binding fashion of NH₂ moieties is noticeably different for all these compounds (*cf.* crystal structure above). But there are differences, too. For example: (i) the highest-wavenumber NH stretching absorption redshifts from 3360 cm⁻¹ typical of LiAB to 3354 cm⁻¹, (ii) the intermediate-wavenumber band blueshifts from 3319 cm⁻¹ typical of LiAB to 3326 cm⁻¹, (iii) the highest-intensity BH stretching band at 2211 cm⁻¹ is in between those for LiAB (2194 cm⁻¹) and NaAB (2289 cm⁻¹), (iv) the major BN stretching absorption shifts significantly from 1448–1478 cm⁻¹ typical of single-cation amidoboranes to 1381 cm⁻¹, (v) the BH deformation region is affected with a violet-shift of the main absorption from 1173–1178 cm⁻¹ typical of single-cation amidoboranes to 1191 cm⁻¹, and more.

The differences in the IR spectra are mostly in the BN stretching, BH stretching and BH deformation regions, which suggests that the BN and BH bonds are the most sensitive spectroscopic markers of the structural differences between LiAB, NaAB and LiNa(AB)₂.

Evolution of the IR spectra of NaLiAB₂ upon heating (ESI[†]) indicates progressive loss of hydrogen and ammonia; the thermally decomposed sample contains nearly no H atoms attached to N (note the absence of the NH stretching band) and all remaining H is attached to B (the BH stretching band is weaker, but detectable).

The weak characteristic triplet centered at 3380 cm⁻¹ appearing in the IR spectra of NaAB alone but *absent* for LiAB and for NaLi(AB)₂ (ESI[†]) is worthy of comment. It has been assigned to an ammonia molecule coordinated to a Na⁺ cation contained in the [Na(NH₃)⁺][NH₂(BH₃)₂⁻] impurity formed from the NaAB product and some unreacted AB during milling.¹⁰ A redshift of the NH stretching band is expected upon coordination of ammonia to a stronger Lewis acid (electron withdrawing moiety) than Na⁺, with Li⁺ as an obvious candidate. However, the DFT calculations suggest the redshift of the IR-active NH stretching frequencies by only 10 cm⁻¹ upon Na⁺ ↔ Li⁺ substitution which excludes the possibility that the weak 3330–3337–3354 cm⁻¹ triplet in the IR spectra of the as-prepared NaLi(AB)₂ (ESI[†]) originates from the Li(NH₃)⁺ cation. The joint experimental and theoretical results thus suggest the absence of [Li⁺...NH₃] and [Na⁺...NH₃] complexes in the as-prepared NaLi(AB)₂. Nevertheless, an eminent band at 3410 cm⁻¹ appears in the FTIR spectrum of NaLi(AB)₂ heated to 50–70 °C and it disappears on subsequent heating to 110 °C. Since the degenerate stretching NH mode of ammonia is found at 3444 cm⁻¹ and it redshifts upon coordination to Lewis acids, we conclude that the band at 3410 cm⁻¹ corresponds to ammonia molecule(s) weakly coordinated to the Na⁺ cation.

The results described above suggest that the efficiencies of the secondary reactions:



are different for each of the three seemingly similar chemical systems (M = Na, Li, Na_{0.5}Li_{0.5}). This is important since the presence of the M(NH₃)⁺-containing impurities must contribute to the facile elimination of the NH₃ impurity of H₂ during

thermal decomposition of amidoboranes (see the next section). Conceivably, the amount of [M(NH₃)⁺][NH₂(BH₃)₂⁻] impurity in the amidoborane specimen crucially depends on the selection of the synthetic method (wet-dry), the purity of starting reagents, the presence of a small excess of ammonia scavengers (LiH or NaH), the type of mill material, the temperature at which the reaction proceeds, or even catalytic amounts of related ammonium (H⁺...NH₃) salts. This surmise helps to rationalize the fact that the amount of ammonia detected in H₂ gas evolved from amidoborates is sometimes very large¹⁰ and sometimes very small.⁵¹

3. Thermal decomposition and impurities of H₂ gas

When heated to 75 °C, NaLi(AB)₂ decomposes without melting, while yielding a white puffy solid, very different in appearance from the lightweight sponge produced by the thermal decomposition of ammonia borane; when heated at 1 K min⁻¹ NaLi(AB)₂ decomposes already at 58 °C. The X-ray diffractogram of NaLi(AB)₂ heated above 110 °C (Fig. 1) consists only of weak reflections from the WC impurity and a broad hump characteristic for amorphous phases.

NaLi(AB)₂ decomposes in two steps (Fig. 5) over the temperature range 75–200 °C, similarly to LiAB and NaAB. The first step (75–110 °C) results in a 6.0% mass loss with a highly exothermic DSC peak at 99 °C. The second step (130–200 °C) is broad and results in a 3.0% mass loss. An endothermic process preceding thermal decomposition can be observed in the temperature range 55–75 °C. This weakly endothermic DSC peak with a maximum at 63 °C does not correspond to melting or a crystalline–crystalline phase transition of the main NaLi(AB)₂ component, as confirmed by our temperature-resolved X-ray studies and by visual observations of a large amount of the sample. Judging from the FTIR spectra (see the preceding section) a portion of NaLi(AB)₂ undergoes amorphization at 50–70 °C yielding a form containing M(NH₃)⁺ cations. The endothermic feature preceding thermal decomposition is characteristic for Na and Li amidoboranes. The nature of this process was discussed previously, suggesting

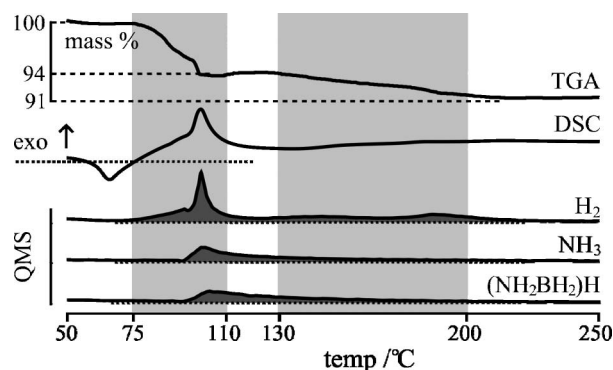


Fig. 5 Thermal decomposition of LiNa(AB)₂ at 10 K min⁻¹: TGA and DSC profile (top); H₂, NH₃, and NH₂BH₃ ion current (bottom). The temperature range shown was cropped to 50–250 °C for better exposition of data. The first and second broad step of decomposition are marked with gray fields. Note that absolute intensities of MS signals are not directly proportional to the amount of H₂ and N-impurities due to different ionization cross-sections of various molecules for the 40 eV electron beam.

Table 3 Hydrogen and nitrogen content of three NaAB samples: as-obtained (25 °C) and heated to 110 °C and 250 °C (average from two independent measurements is given); theoretical data for the as-obtained sample calculated according to the chemical formula are also shown

Element	Theory	NaLi(AB) ₂		
		25 °C	110 °C	250 °C
H	11.1%	10.9%	6.5%	4.1%
N	31.1%	27.9%	26.0%	28.5%

presence of intermolecular transformation leading to the evolution of ammonia.¹⁰

Infrared and mass spectroscopic analyses of the evolved gas show evolution of H₂ contaminated with both ammonia as well as a protonated form of the volatile NH₂BH₂ as in the case of LiAB²¹ and NaAB.¹⁰

The total mass loss of NaLi(AB)₂ (9.0%) is intermediate between the values reported for single-cation amidoboranes: LiAB (10.9%) and NaAB (6.6–7.5%).^{8–10} It is also smaller than the theoretical gravimetric hydrogen capacity (11.1%) of NaLi(AB)₂ which in the first approximation suggests that *ca.* 1/5 of the total hydrogen content remains in the amorphous solid left after thermal decomposition. The situation is, however, more complex.

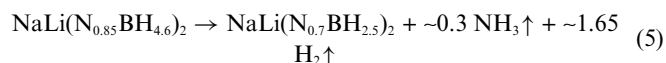
Elemental analysis of NaLi(AB)₂ and the products of its thermal decomposition confirm the evolution of hydrogen and some amount of ammonia upon heating (Table 3). Comparison of the experimental data for the as-obtained sample with the theoretical values shows a decrease of nitrogen content, suggesting that traces of ammonia are evolved already during milling, similarly as in the case of NaAB.¹⁰ Heating to 110 °C results in loss of both hydrogen and nitrogen. Further heating to 250 °C results mostly in loss of hydrogen. These results are consistent with EGA (Fig. 5); recollect that evolution of hydrogen and ammonia is observed in the first step of decomposition, while above 110 °C no ammonia is detected in the gases evolved.

Quantitative considerations based on N and H content *via* solution of a system of two linear equations show that already during milling about one ammonia molecule per three formula units of NaLi(AB)₂ is evolved:

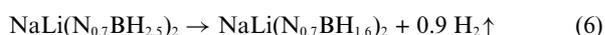


The stoichiometric formula of NaLi(N_{0.85}BH_{4.6})₂ reflects the total elemental content of the sample but it should be remembered that atomic coefficients are likely arithmetic averages of those for crystalline stoichiometric NaLi(NBH₂)₂ (*cf.* XRD) and of amorphous unidentified NaLi(N_{0.7}BH_{4.2})₂ residue.

In the first step of decomposition (75–110 °C), evolution of hydrogen and ammonia is observed:



while in the second decomposition step (130–200 °C) nearly pure hydrogen is evolved:



The amorphous product of decomposition at 250 °C contains about 3/4 of the initial N content and about 3/4 of the initial H content of NaLi(AB)₂, and its chemical formula may be approximated as NaLiN_{1.4}B₂H_{3.2}.

Conclusions

We have succeeded in the preparation and characterization of the first mixed-cation amidoborane derivative, Na[Li(NH₂BH₃)₂], with large theoretical H content (as high as 11.1 wt% – gravimetric, and 114.4 g l⁻¹ – volumetric) exceeding the DOE targets. The crystal structure was solved yielding a centrosymmetric triclinic cell with two formula units inside the unit cell (*Z* = 2). Na[Li(NH₂BH₃)₂] is a rare example of an inorganic sodium–lithium compound with a unique crystal structure, containing polymeric [Li(AB)₂]⁻₂ anions separated by isolated Na⁺ cations. Na[Li(NH₂BH₃)₂] is thus a genuine pseudoternary ionic salt and not a mixture or solid solution of LiNH₂BH₃ and NaNH₂BH₃, thus confirming the rule that the properties of bimetallic (pseudoternary) systems are usually not a simple superposition of the properties of single-cation (pseudobinary) components.

Na[Li(NH₂BH₃)₂] decomposes exothermally in the temperature range 75–110 °C, while releasing 6.0 wt% of hydrogen, and an additional 3.0 wt% upon further heating to 200 °C. The hydrogen evolved is contaminated with ammonia as in the case of sodium and lithium amidoborane.¹⁰ The [Na⁺ ... NH₃] cation-containing impurity is absent in the as-prepared LiNa(AB)₂, but it appears in the sample upon endothermic (partial) amorphization at 50–70 °C as judged from the IR absorption spectra. This impurity, analogous to the sodium-containing one present in the samples of NaAB ([Na(NH₃)⁺][NH₂(BH₃)₂⁻],¹⁰ *i.e.* an analogue of the [NH₄⁺][NH₂(BH₃)₂] form of ammonia borane) is charged responsible for the emission of ammonia during the thermal decomposition of Na[Li(NH₂BH₃)₂].

Note added in proof

See ref. 52 for a recent important study by Kang *et al.* which reports the synthesis and characterization of sodium–magnesium mixed-cation amidoborane: NaMg(AB)₃.

Acknowledgements

Authors would like to thank to Mr Andrew Churchard, M. Res, and the entire LTNFM staff, for help. This research was funded from 37/6PR UE/2007/7 grant of the Polish Ministry of Science and Higher Education. PhD fellowship for R.V.G. and access to the TGA-DSC-EGA analyzer was provided by Marie Curie Research Training Network ‘Hydrogen’ (EU 6th FP, MRTNCTT-2006–032474). The authors acknowledge SNBL for in-house beamtime allocation.

Notes and references

- 1 S. G. Shore and R. W. Parry, *J. Am. Chem. Soc.*, 1955, **77**, 6084.
- 2 J. Baumann, E. Baitalow and G. Wolf, *Thermochim. Acta*, 2005, **430**, 9; see also recent reviews: C. W. Hamilton, R. T. Baker, A. Staibitz and I. Manners, *Chem. Soc. Rev.*, 2009, **38**, 279; H.-L. Jiang, K. Singh, J.-M. Yan, X.-B. Zhang and Q. Xu, *ChemSusChem*, 2010, **3**, 541.
- 3 H. I. Schlesinger and A. B. Burg, *J. Am. Chem. Soc.*, 1938, **60**, 290.
- 4 P. M. Niedenzu, Ph.D. *Dissertation*, The Ohio State University, 1990.
- 5 T. Salupo, Ph.D. *Dissertation*, The Ohio State University, 1993.
- 6 A. L. DeGraffenreid, Ph.D. *Dissertation*, The Ohio State University, 1995.
- 7 A. G. Myers, B. H. Yang and D. J. Kopecky, *Tetrahedron Lett.*, 1996, **37**, 3623.

- 8 Z. Xiong, C. K. Yong, G. Wu, P. Chen, W. Shaw, A. Karkamkar, T. Autrey, M. O. Jones, S. R. Johnson, P. P. Edwards and W. I. F. David, *Nat. Mater.*, 2008, **7**, 138.
- 9 Z. Xiong, G. Wu, Y. S. Chua, J. Hu, T. He, W. Xu and P. Chen, *Energy Environ. Sci.*, 2008, **1**, 360.
- 10 K. J. Fijalkowski and W. Grochala, *J. Mater. Chem.*, 2009, **19**, 2043.
- 11 H. V. K. Diyabalanage, T. Nakagawa, R. P. Shrestha, T. A. Semelsberger, B. L. Davis, B. L. Scott, A. K. Burrell, W. I. F. David, K. R. Ryan, M. Owen Jones and P. P. Edwards, *J. Am. Chem. Soc.*, 2010, **132**, 11837.
- 12 Q. Zhang, Ch. Tang, Ch. Fang, F. Fang, D. Sun, L. Ouyang and M. Zhu, *J. Phys. Chem. C*, 2010, **114**, 1709.
- 13 H. V. K. Diyabalanage, R. P. Shrestha, T. A. Semelsberger, B. L. Scott, M. E. Bowden, B. L. Davis and A. K. Burrell, *Angew. Chem., Int. Ed.*, 2007, **46**, 8995.
- 14 J. Spielmann, G. Jansen, H. Bandmann and S. Harder, *Angew. Chem., Int. Ed.*, 2008, **47**, 6290.
- 15 R. V. Genova, K. J. Fijalkowski, A. Budzianowski and W. Grochala, *J. Alloys Compd.*, 2010, **499**, 144.
- 16 J. M. Hoy, *Master's Thesis*, The Ohio State University, 2010.
- 17 S. Haider, Ph.D. *Dissertation*, Queen Mary University of London, 2005.
- 18 Y. S. Chua, G. Wu, Z. Xiong, A. Karkamkar, J. Guo, M. Jian, M. W. Wong, T. Autrey and P. Chen, *Chem. Commun.*, 2010, **46**, 5752.
- 19 Y. Zhang, K. Shimoda, T. Ichikawa and Y. Kojima, *J. Phys. Chem. C*, 2010, **114**, 14662.
- 20 DeGraffenried used an ammonia trap during thermal decomposition of KAB, so ammonia could not be detected; Diyabalanage observed pure hydrogen. Salupo (ref. 5) did not investigate thermal decomposition of Eu(AB)₂ and Yb(AB)₂.
- 21 Lithium amidoborane also releases ammonia during thermal decomposition (cf. ESI†).
- 22 F. A. Uribe, S. Gottesfeld and T. A. Zawodzinski Jr, *J. Electrochem. Soc.*, 2002, **149**, A193; N. Rajalakshmi, T. T. Jayanth and K. S. Dhathathreya, *Fuel Cells*, 2004, **3**, 177.
- 23 W. Grochala and P. P. Edwards, *Chem. Rev.*, 2004, **104**, 1283.
- 24 M. H. Sorby, H. W. Brinks, A. Fossdal, K. Thorshaug and B. C. Hauback, *J. Alloys Compd.*, 2006, **415**, 284.
- 25 L. Jeloaić, J. Zhang, F. Cuevas, M. Lacroche and P. Raybaud, *J. Phys. Chem. C*, 2008, **112**, 18598.
- 26 F. H. Wang, Y. F. Liu, M. X. Gao, K. Luo, H. G. Pan and Q. D. Wang, *J. Phys. Chem. C*, 2009, **113**, 7978.
- 27 E. A. Nickels, M. O. Jones, W. I. F. David, S. R. Johnson, R. L. Lowton, M. Sommariva and P. P. Edwards, *Angew. Chem., Int. Ed.*, 2008, **47**, 2817.
- 28 H. Hagemann, M. Longhini, J. W. Kaminski, T. A. Wesolowski, R. Černý, N. Penin, M. H. Srrby, B. C. Hauback, G. Severa and C. M. Jensen, *J. Phys. Chem. A*, 2008, **112**, 7551.
- 29 Y. Filinchuk, D. Chernyshov and V. Dmitriev, *Z. Kristallogr.*, 2008, **223**, 649.
- 30 A. P. Hammersley, S. O. Svensson, M. Hanfland, A. N. Fitch and D. Häusermann, *High Pressure Res.*, 1996, **14**, 2358.
- 31 Accelrys, Inc (2007). *Materials Studio 4*, Accelrys, Inc., San Diego, USA.
- 32 P. E. Werner, L. Eriksson and M. Westdahl, *J. Appl. Crystallogr.*, 1985, **18**, 367.
- 33 J. W. Visser, *J. Appl. Crystallogr.*, 1969, **2**, 89.
- 34 M. Neumann, *J. Appl. Crystallogr.*, 2003, **36**, 356.
- 35 A X S Bruker (2009): *TOPAS 4.2 User manual*, Bruker A X S GmbH, Karlsruhe, Germany.
- 36 A. A. Coelho, *J. Appl. Crystallogr.*, 2003, **36**, 86.
- 37 G. S. Pawley, *J. Appl. Crystallogr.*, 1981, **14**, 357.
- 38 A. Le Bail, H. Duroy and J. L. Fourquet, *Mater. Res. Bull.*, 1988, **23**, 447.
- 39 J. Bergmann, R. Kleeberg, A. Haase and B. Breidenstein, *Mater. Sci. Forum*, 2000, **347–349**, 303.
- 40 A. Boulitif and D. Louer, *J. Appl. Crystallogr.*, 2004, **37**, 724.
- 41 V. Favre-Nicolin and R. Černý, *J. Appl. Crystallogr.*, 2002, **35**, 734.
- 42 A. Spek, *Acta Cryst. A*, 1990, **46**, C34.
- 43 H. M. Rietveld, *Acta Crystallogr.*, 1967, **22**, 151; H. M. Rietveld, *J. Appl. Crystallogr.*, 1969, **2**, 65.
- 44 R. J. Hill and C. J. Howard, *J. Appl. Crystallogr.*, 1987, **20**, 467.
- 45 P. E. Blöchl, *Phys. Rev. B*, 1994, **50**, 17953; G. Kresse and D. Joubert, *Phys. Rev. B*, 1999, **59**, 1758.
- 46 G. Kresse, J. Furthmüller, *Software V A SP*, Vienna (1999); G. Kresse, J. Furthmüller, *Phys. Rev. B*, 1996, **54**, 11169G. Kresse, J. Furthmüller, *Comput. Mater. Sci.* 1996, **6**, 15.
- 47 An unidentified P1 impurity has very small unit cell volume, $V = 68.618 \text{ \AA}^3$, typical of simple stoichiometric formulas (e.g. NaH has volume per formula unit of ca. 29 \AA^3). Its content increases in samples left for a few days in the argon atmosphere.
- 48 The difference of 3.75 \AA^3 between the volume per formula unit of LiNa(AB)₂ and pseudobinary amidoboranes corresponds to an entropy difference of $\Delta S = 6.59 \text{ J mol}^{-1} \text{ K}^{-1}$, which is equivalent to a slight entropic stabilization of LiNa(AB)₂ with respect to its substrates by a (ΔS T) factor of 2.0 kJ mol^{-1} at room temperature. Cf. H. D. B. Jenkins and L. Glasser, *Inorg. Chem.*, 2003, **42**, 8702.
- 49 Z. Zák and M. Kosicka, *Acta Crystallogr. Sect. B*, 1978, **34**, 38.
- 50 The mixed Li and Na (1:1) compounds are actually rare; the following ones were structurally characterized according to In-formatica structural database (Medea): NaLiCO₃ (3 polymorphs), NaLiSO₄, NaLi(HCOO)₂·xH₂O, NaLiCdS₂, NaLiY₂F₈ (2 polymorphs), NaLiZnO₂, NaLiZnP₂O₇, Na₂Li₂Ti₆O₁₄, and mineral, Na₄Li₄Al₆Si₆S_{2.05}O_{24.85}H_{1.7}.
- 51 A. T. Luedtke and T. Autrey, *Inorg. Chem.*, 2010, **49**, 3905.
- 52 X. Kang, J. Luo, Q. Zhang and P. Wang, *Dalton Trans.*, 2011, DOI: 10.1039/c0dt00835d, in press.